

# Conformal Anomaly and Critical Exponents of the $XY$ -Ising model

M.P. Nightingale

*Department of Physics, University of Rhode Island,  
Kingston, Rhode Island, 02881.*

E. Granato

*Laboratório Associado de Sensores e Materiais,  
Instituto Nacional de Pesquisas Espaciais,  
12 225 São José dos Campos, São Paulo, Brazil.*

J.M. Kosterlitz

*Department of Physics, Brown University,  
Providence, Rhode Island, 02902.*

## Abstract

We use extensive Monte Carlo transfer matrix calculations on infinite strips of widths  $L$  up to 30 lattice spacing and a finite-size scaling analysis to obtain critical exponents and conformal anomaly number  $c$  for the two-dimensional  $XY$ -Ising model. This model is expected to describe the critical behavior of a class of systems with simultaneous  $U(1)$  and  $Z_2$  symmetries of which the fully frustrated  $XY$  model is a special case. The effective values obtained for  $c$  show a significant decrease with  $L$  at different points along the line where the transition to the ordered phase takes place in a single transition. Extrapolations based on power-law corrections give values consistent with

$c = 3/2$  although larger values can not be ruled out. Critical exponents are obtained more accurately and are consistent with previous Monte Carlo simulations suggesting new critical behavior and with recent calculations for the frustrated  $XY$  model.

## I. INTRODUCTION

Recently, the critical behavior of the two-dimensional  $XY$ -Ising model, consisting of  $XY$  and Ising models coupled through their energy densities, has been studied in some detail<sup>1,2</sup>. The model is expected to describe the critical behavior of a class of systems with  $U(1)$  and  $Z_2$  symmetries which includes, for example, two-dimensional fully frustrated  $XY$  (FFXY) models<sup>3,4,5,6,7,8,9,10,11,2,12,13,14</sup>, or alternatively, two-dimensional arrays of Josephson junctions<sup>15</sup>, one-dimensional ladders of Josephson junctions with charging effects<sup>16</sup>, helical  $XY$  models<sup>7</sup> and some surface solid-on-solid models<sup>17,18</sup>. The  $XY$ -Ising model is also of great theoretical interest in its own right as the phase diagram obtained by Monte Carlo simulations gave rise to interesting and unusual critical behavior<sup>1</sup>. Recent work by Knops *et al.*<sup>14</sup> has further justified the relation between  $XY$ -Ising and FFXY models by showing that the phase coupling across chiral domains in the FFXY model is irrelevant at criticality. In the subspace of parameters of the model where the  $XY$  and Ising coupling constants have the same magnitude, separate  $XY$  and Ising transitions, first-order transitions and a critical line with simultaneous  $XY$  and Ising ordering were found.

The numerical study revealed that starting at the branch point where separate  $XY$  and Ising transitions merge, the line of single transitions has a segment of continuous transitions which eventually become first order as one moves away from the branch point. Along the segment of continuous transitions, the critical exponents associated with the Ising-like order parameter were found to be significantly different from the pure Ising values and, in fact, appeared to be non-universal, varying along the line. Besides by critical exponents, this critical line was also characterized by its central charge, or conformal anomaly number  $c$ . The central charge was estimated from the finite-size scaling of the free energy of infinite strips at criticality, obtained from Monte Carlo Transfer Matrix calculations. The results obtained from strips of width up to  $L = 12$  lattice spacing were rather surprising: the central charge appears to increase continuously along this line, from  $c \approx 1.5$  close to the branch point to  $c \approx 2$  near the tricritical point.

Similar calculations<sup>11,19,13</sup> of the critical exponents and central charge for the FFXY model were consistent with these results. Although models with varying  $c$  are well known, as for example the  $q$ -state Potts and  $O(n)$  models with a continuously varying number of states  $q$  and  $n$ , the behavior for XY-Ising model is rather unexpected since, contrary to the previous models, the transfer matrix can be chosen symmetric and along the critical line a parameter is changing that does not affect the symmetry. The question then arises if this behavior is a real effect or an artifact due to limited strip widths. In view of the relation between the XY-Ising and FFXY models, the answer to this question may also give some insight into the behavior of the central charge for FFXY models<sup>20,11,13,14</sup>. Also, it is important to have improved estimates for the critical exponents in order to be more certain about the non-Ising nature of the critical behavior along the line of single transitions.

In this work we report the results of extensive Monte Carlo transfer matrix calculations, using infinite strips of widths  $L$  up to 30 lattice spacing, aimed to resolve some of the issues raised by previous calculations on the XY-Ising model. Rather than attempting to evaluate critical exponents and central charge at several different points along the line of single transitions to check if these quantities do change or remain constant along the critical line, we have concentrated on a couple of points but performed extensive calculations for large  $L$  and used variance reduction techniques to decrease the statistical errors. The results for the effective value of  $c$  show a significant decrease with increasing  $L$ , indicating that they even the extrapolated estimates have not yet reached their asymptotic values for  $L = 30$ , the largest strip width considered. Extrapolation suggests values not inconsistent with  $c = 3/2$ . However, on purely numerical grounds, we can not rule out the possibility of a larger value or even a varying  $c$  along the line. Our results for the central charge suggest that the recent estimates of this quantity,  $c \approx 1.6$  for the related FFXY models<sup>11,16,13,14</sup> are likely to be subject to similar systematic errors due to slowly decaying corrections to scaling and the asymptotic value is in fact consistent with  $c = 3/2$ . The critical exponents associated with Ising-like order parameter are obtained more accurately, although there are some puzzling inconsistencies. The exponents are found to be significantly different from the

pure Ising values but consistent with the previous Monte Carlo simulations which suggested new critical behavior<sup>1</sup> and recent estimates for the FFX $Y$  model using Monte Carlo<sup>13</sup> and exact numerical transfer matrix calculations<sup>14</sup>.

The paper is organized as follows. In Sec. II, we define the model and briefly review the main features of its phase diagram, indicating the locations near the phase boundary where the Monte Carlo transfer matrix calculations were performed. In Sec. III we provide details on the Monte Carlo transfer matrix method and the implementation of the variance reduction techniques. In Sec. IV, a finite-size scaling analysis of the interfacial free energy is used to extract critical quantities. In Sec. V, we present the numerical results for critical couplings, exponents and central charge and in Sec. VI we discuss and compare these results with previous calculations. Finally, Sec. VI is devoted to the conclusions and final remarks.

## II. MODEL AND PHASE DIAGRAM

The  $XY$ -Ising model is defined by the following Hamiltonian<sup>1,2</sup>

$$\frac{H}{kT} = - \sum_{\langle ij \rangle} [(A + Bs_i s_j) \mathbf{n}_i \cdot \mathbf{n}_j + Cs_i s_j], \quad (1)$$

where  $s = \pm 1$  is an Ising spin and  $\mathbf{n} = (\cos \theta, \sin \theta)$  is a two-component unit vector, is an  $XY$  spin. The model can be regarded as the infinite coupling limit,  $h \rightarrow \infty$ , of two  $XY$  models<sup>6,7,8</sup> coupled by a term of the form  $h \cos 2(\theta_1 - \theta_2)$  and has a rich phase diagram in the  $A, B$  plane that depends strongly on the value of  $C$ . The model with  $A \neq B$  is relevant for the anisotropic frustrated  $XY$  model<sup>8</sup> and anti-ferromagnetic restricted solid-on-solid model<sup>17</sup>.

In this work we will be concerned with the critical behavior of the  $XY$ -Ising model of Eq. (1), defined on a square lattice, in the subspace  $A = B$ ,

$$\frac{H}{kT} = - \sum_{\langle ij \rangle} [A(1 + s_i s_j) \mathbf{n}_i \cdot \mathbf{n}_j + Cs_i s_j], \quad (2)$$

which is relevant for the isotropic frustrated  $XY$  model or its one-dimensional quantum version<sup>16</sup>. The phase diagram obtained by Monte Carlo simulations is shown in Fig. 1 and

consists of three branches joining at  $P$ , in the ferromagnetic region  $A > 0$ ,  $A + C > 0$ . One of the branches corresponds to a single transition with simultaneous loss of  $XY$  and Ising order and the other two to separate Kosterlitz-Thouless (KT) and Ising transitions. An important feature of the phase diagram is that there is no phase with Ising disorder and  $XY$  order thus indicating that Ising disorder induces also  $XY$  disorder in this model. This is related to the special symmetry under the transformation

$$\mathbf{n}_j \rightarrow s_j \mathbf{n}_j \tag{3}$$

which holds if  $A = B$ , since  $XY$  spins are not coupled across an Ising domain wall where  $s_i s_j + 1 = 0$ . The behavior of FFX $Y$  model corresponds to the behavior of this model along a particular path through this phase diagram. The available numerical results for the standard FFX $Y$  model<sup>1,19,13,14</sup> are consistent with a single transition but generalized versions could correspond to a path through the double transition region. In fact, a Coulomb-gas representation of the FFX $Y$  model with an additional coupling between nearest neighbor vortices has a phase diagram with identical structure<sup>10</sup>. In the one-dimensional quantum version of the frustrated  $XY$  model<sup>16</sup>, related to the zero-temperature transition of Josephson-junction ladders, double or single transitions will result depending on the ratio between inter-chain and intra-chain couplings. In the Monte Carlo simulations<sup>2</sup>, the critical line  $PT$  in Fig. 1 appears to be non-universal as the critical exponents associated with the Ising order parameter were found to vary systematically along this line. In addition, a preliminary evaluation of the central charge<sup>1</sup>  $c$  using data for the free energy of infinite strips obtained from Monte Carlo transfer matrix appeared to indicate that  $c$  varies from  $c \approx 1.5$  near  $P$  to  $c = 2$  near  $T$ . These results for the central charge were based on strips of width  $L$  up to 12 lattice spacings. However, this range of  $L$  and the numerical noise in the data does not allow one to extrapolate to the large  $L$  limit and these estimates are thus subject to systematic errors. To obtain accurate estimates it is necessary to perform calculations for larger  $L$  and also to reduce the errors. Rather than attempting to evaluate  $c$  at several different points along the line  $PT$  in order to check if this quantity changes or remains constant along the line, we have

concentrated our attention at a few points but performed extensive calculations for large  $L$  and used variance reduction techniques to decrease the errors. The calculations discussed in the following sections were performed primarily along the cuts through the critical line as indicated in Fig. 1.

### III. MONTE CARLO TRANSFER MATRIX

Estimates of the free energy density per lattice site was computed using the Monte Carlo transfer matrix method. We give a brief summary of the essentials of this method and refer the reader to Ref. 21 for more details.

Helical boundary conditions are convenient for these computations. In this case the transfer matrix can be chosen to be a sparse matrix for the case where one matrix multiplication corresponds to the addition of one surface site to the lattice, as illustrated in Fig. 2. The sparseness follows from the fact that from any given configuration of surface sites only those new configurations can be reached that differ at that newly added site only. We used a transfer matrix defined by

$$T(s_1, \dots, s_L; \mathbf{m}_1, \dots, \mathbf{m}_L | t_1, \dots, t_L; \mathbf{n}_1, \dots, \mathbf{n}_L) = \quad (4)$$

$$e^{(A\mathbf{n}_{L-1}\cdot\mathbf{n}_L + B\mathbf{n}_{L-1}\cdot\mathbf{n}_L t_{L-1} t_L + C t_{L-1} t_L + A\mathbf{n}_L\cdot\mathbf{m}_1 + B\mathbf{n}_L\cdot\mathbf{m}_L s_1 + C s_{L-1} s_L)} \prod_{k=2}^L \delta(\mathbf{m}_k - \mathbf{n}_{k-1}) \delta_{s_k, t_{k-1}}.$$

The statistical variance of transfer matrix Monte Carlo computations is proportional to the variance of the quantity

$$\mu = \sum_{s_1} \int d/\mathbf{b}\mathbf{f}\mathbf{m}_1 T(s_1, \dots, s_L; / \mathbf{b}\mathbf{f}\mathbf{m}_1, \dots, \mathbf{m}_L | t_1, \dots, t_L; \mathbf{n}_1, \dots, \mathbf{n}_L). \quad (5)$$

The variance can be reduced by applying the transfer matrix algorithm to a similarity transform  $\hat{T}$  of the transfer matrix  $T$  defined in Eq. (5). The transformation requires an optimized trial eigenvector  $\psi_T$  and is defined as follows:

$$\hat{T}(\{s\}; \{\mathbf{m}\} | \{t\}; \{\mathbf{n}\}) = \psi_T(\{s\}; \{\mathbf{m}\}) T(\{s\}; \{\mathbf{m}\} | \{t\}; \{\mathbf{n}\}) / \psi_T(\{t\}; \{\mathbf{n}\}) \quad (6)$$

where  $\{x\} \equiv x_1, \dots, x_L$ .

In the ideal case, when  $\psi_T$  is an exact left eigenvector, the local eigenvalue  $\hat{\mu}$ , defined by Eq. (5) with  $T$  replaced by  $\hat{T}$ , is a constant - an eigenvalue of the transfer matrix. In practice, the better the quality of the trial function, the smaller the statistical noise in the Monte Carlo estimates of the transfer matrix eigenvalues.

For the design of good trial states it is helpful to realize that the dominant left eigenvector is proportional to the conditional partition function of a semi-infinite lattice, extending to infinity towards the left, as indicated in Fig. 2, conditional on the microscopic state of the surface.

Our computations used the following form for the trial vectors:

$$\psi_T(s_1, \dots, s_L; \mathbf{n}_1, \dots, \mathbf{n}_L) = \exp \left( \sum_{i,j}^* (A_{i,j} \mathbf{n}_i \cdot \mathbf{n}_j + B_{i,j} \mathbf{n}_i \cdot \mathbf{n}_j s_i s_j + C_{i,j} s_i s_j) \right). \quad (7)$$

Here the parameters  $A_{ij}$ ,  $B_{ij}$ , and  $C_{ij}$  are variational parameters, which are chosen so as to minimize the variance of  $\hat{\mu}$ , as described in detail in Ref. 21. In the expression (7) the asterisk indicates that the sum over the pairs of surface sites labeled  $i$  and  $j$  is truncated, as is required for computational efficiency. To truncate in a way that allows systematic improvement of the quality of the trial function, it is necessary to guess for which pairs of sites  $i$  and  $j$  the interaction parameters  $A_{i,j}$  in Eq. (7) have the largest magnitudes, and similarly for  $B_{i,j}$ , and  $C_{i,j}$ . Obviously, interaction strengths will decay with distance, but owing to the helical boundary conditions and the surface defect, the geometrical distance is not quite correct. Instead, a distance can be defined between surface sites  $i$  and  $j$  of the semi-infinite strip (illustrated in Fig. 2) as the length of the shortest path that: (a) connects sites  $i$  and  $j$ ; (b) passes only through bulk sites (indicated by full circles in Fig. 2); and (c) travels along the edges of the square lattice.

The reason for excluding surface sites from the path is that the correlations described by the interaction parameters  $A_{ij}$ , *etc.* are mediated only via bulk sites, since those are the only ones that contain variables that are not frozen in the conditional partition function. Fig. 2 shows a path of length three. Owing to the presence of the surface defect no two paths are strictly equivalent and, since the surface interactions can be regarded as functions



of the minimal path defined above, all parameters have to be assumed different. However, the transformed transfer matrix  $\hat{T}$  depends only on the ratio of the values of two trial states shifted by a single lattice unit along the surface. By artificially imposing translational invariance on the interaction parameters, one can produce cancellations in the computation. This reduces the number of arithmetic operations from order  $L$  (in the absence of translation symmetry) to a number of the order of the maximum path length at which the interaction are truncated.

Suppose that interactions in the trial function are truncated at path length  $l$ , measured in units of the lattice spacing, then the following compromise seems to work satisfactorily: give those interaction parameters the same values that are (a) farther away from the defect than  $l$ , and (b) would be equivalent by translation symmetry in the case of simple periodic boundary conditions. In particular, this means that all interactions associated with paths that cross the defect are allowed to be different in the computation. It should be noted that this approximation can only be improved to a point: as soon as many-body interactions appear that are of greater strength than pair interactions included in the trial function, ignoring the many-body interactions makes it impossible and pointless to determine the two-body interactions.

We are interested only in studying the behavior of systems with  $B = C$ , but the twisted boundary conditions force us also to consider the case where  $B = -C$ , which is obtained by inverting either the Ising or the  $XY$  variables on one sub-lattice. In all of these cases we used trial functions in which the corresponding relation was maintained between the interaction parameters appearing in the trial vector, Eq. (7), i.e.,  $B_{ij} = C_{ij}$  if  $i$  and  $j$  belong to the same sub-lattice and  $B_{ij} = -C_{ij}$  otherwise or if twisted boundary conditions are used.

As a final comment we mention that by using the variance reduction scheme mentioned above the Monte Carlo calculation can be accelerated roughly by a factor of two hundred<sup>22</sup>.

#### IV. FINITE-SIZE SCALING

To locate the critical couplings and determine the critical exponents we will do a finite-size scaling analysis of interfacial free energies. Since the model contains both  $XY$  and Ising variables, there are in principle two types of interfacial free energies that can be determined by a suitable choice of the boundary conditions. If a twist in the Ising variables is imposed by anti-periodic boundary conditions, a domain wall is forced along the infinite strip and the associated interfacial free energy can be obtained from the difference per surface unit the free energies of systems with periodic and anti-periodic boundary conditions. On the other hand, if the same procedure is followed for the  $XY$  variables, a smooth phase twist of  $\pi$  is forced across the infinite strip. The transfer matrix calculations are done for an  $L \times \infty$  strip with  $L$  even and helical boundary conditions. With this set-up, it is simple to introduce independent twists in the Ising and  $XY$  degrees of freedom.

The interfacial free energy of an Ising domain wall of length  $L$  along the strip is given by

$$\Delta F_{\text{I}} = L^2[f(A, A, C) - f(A, -A, -C)], \quad (8)$$

where  $f(A, B, C)$  is the free energy per site of the  $XY$ -Ising model of Eq. (1). The parameters  $A$  and  $C$  are chosen so that the ground state is ferromagnetic,  $A > 0$  and  $A + C > 0$ , so that taking  $B \rightarrow -B = -A$  induces a domain wall between the two anti-ferromagnetic Ising ground states. Similarly, a twist of  $\pi$  in the  $XY$  degrees of freedom is induced by  $A \rightarrow -A$  and  $B \rightarrow -B$  so that

$$\Delta F_{XY} = L^2[f(A, A, C) - f(-A, -A, C)], \quad (9)$$

and the helicity modulus  $\gamma$  is given by

$$\gamma = 2\Delta F_{XY}/\pi^2. \quad (10)$$

At a conventional second-order transition, the interfacial free energy has the simple scaling form

$$\Delta F(A, C; L) = \mathcal{A}(L^{y_T} t), \quad (11)$$

where  $\mathcal{A}(u)$  is a scaling function and  $t(A, C)$  is the non-linear scaling field measuring the distance from the critical point; the thermal scaling exponent  $y_T$  is related by  $\nu = 1/y_T$  to the exponent  $\nu$ , which describes the divergence of the correlation length at criticality. In our analysis, we fix one of the parameters,  $A$  or  $C$ , and expand  $t$  to quadratic order, i.e., for fixed  $C$  we have  $t = A - A_c(C) + k[A - A_c(C)]^2$  and similarly when  $A$  is kept fixed. In the vicinity of the critical coupling  $t = 0$ , a standard finite size scaling expansion in  $u = tL^{y_T}$  for  $u \approx 0$  yields

$$\Delta F(A, C; L) = a_0 + a_1 u + a_2 u^2 + \dots \quad (12)$$

With our convention,  $u$  is positive in the ordered phase,  $\Delta F$  will increase with  $L$  for  $u > 0$ , decrease for  $u < 0$  and be a constant at  $u = 0$  for sufficiently large  $L$  so that corrections to scaling have become negligible.

Sufficiently close to  $u = 0$ , Eq. (12) can be used to obtain accurate estimates of the critical exponent  $y_T$  (or equivalently  $\nu$ ) and the critical values  $A$  and  $C$ . The expansion is truncated at some high order ( $u^5$  in some cases). A critical dimension  $x^{(d)}$  of a disorder operator can be obtained from the constant  $a_0$  via

$$x^{(d)} = \frac{a_0}{2\pi}. \quad (13)$$

The critical dimension  $x$  describes the decay with distance  $r$  at criticality of the two-point correlation function  $g(r)$  of an operator determined by the choice of boundary conditions:  $g(r) \propto r^{-2x^{(d)}}$ . The scaling exponent  $y^{(d)} = 2 - x^{(d)}$  describes the behavior of this operator under scaling.

As mentioned above, we consider two kinds of anti-periodic boundary conditions. Subscripts will be used to distinguish the exponents  $x^{(d)}$  and  $y^{(d)}$  of the associated operators. In the case of anti-periodic boundary conditions in the  $XY$  variables, the conjugate operator is a vortex of strength  $\frac{1}{2}$ , measured in units  $2\pi$ . Such an operator is represented as the end point of a path on the dual lattice:  $XY$  bonds crossing this path have their interactions

changed from  $A$  to  $-A$ . Because of the symmetry of the model under the transformation given in Eq. (3) this operator is equivalent to one where the  $B$  is changed to  $-B$ . The exponents of the  $\frac{1}{2}$ -vortex will be denoted by  $x_{XY,\frac{1}{2}}^{(d)}$  and  $y_{XY,\frac{1}{2}}^{(d)}$ . The operator corresponding to the case of antisymmetric boundary conditions for the Ising variables is the standard Ising disorder operator. The exponents for this case will be denoted  $x_I^{(d)}$  and  $y_I^{(d)}$ . For self-dual models or models for which a renormalization mapping to the Gaussian model exists, the disorder operators can be related to order operators, but we cannot derive either of those properties for the  $XY$ -Ising model.

The critical exponents were estimated by making a scaling plot of  $\Delta F$  in which the parameters were estimated by a constrained least-square fits with the critical couplings fixed at their most reliable estimates, i.e., those obtained by extrapolation from the Ising domain wall data. Unfortunately, the discontinuity in the helicity modulus  $\gamma$  is not accessible by similar finite size scaling considerations since the discontinuity in  $\gamma$  is defined in the thermodynamic limit  $L \rightarrow \infty$  and

$$\Delta\gamma = 2[\mathcal{A}(\infty) - \mathcal{A}(-\infty)]/\pi^2. \quad (14)$$

A rough estimate from Fig. 4 for  $\mathcal{A}(\pm\infty)$  gives  $\Delta\gamma \approx 1.3$  which is about double the value  $2/\pi$  of the two-dimensional  $XY$  model. This estimate is not very reliable but we can say with a considerable degree of confidence that  $\Delta\gamma$  is much larger than  $2/\pi$  in this coupled  $XY$ -Ising model and in the  $FFXY$  model.

In addition to critical exponents, another important quantity which provides information on the nature of the critical behavior is the central charge  $c$  of the conformal invariance. This quantity can be obtained from the amplitude of the singular part of the free energy per site<sup>24</sup>, at criticality, in the infinite strip by

$$f(A_c, C_c, L) \approx f_\infty + \frac{\pi c}{6L^2} \quad (15)$$

for sufficiently large  $L$ , where  $f_\infty$  denotes the regular contribution to the free energy at the critical point. The central charge classifies the possible conformally invariant critical

behaviors. For example, for the pure Ising model,  $c = 1/2$ , and along the critical line of the  $XY$  model  $c = 1$ . Although  $c$  is only defined at criticality, Eq. (15) can be used to define a size and coupling dependent effective central charge  $c(A, C, L)$  away from the critical point. If this quantity is now identified as the function  $c(g)$  defined in the  $c$ -theorem of Zamolodchikov<sup>25</sup>, where  $g$  stands for a set of coupling constants, this quantity should have a well-defined behavior near criticality since, according to the  $c$ -theorem,  $c(g)$  is a monotonically decreasing function under a renormalization group transformation and reaches a constant value equal to the central charge at the fixed point. An interesting consequence of this identification is that  $c(A, C, L)$  should have a maximum near the critical line of single transitions in the  $XY$ -Ising model with a lower bound  $c(A, C, L) \geq 3/2$  and away from the critical line should converge to either  $c(A, C, L) = 1$  in the  $XY$  ordered phase or to  $c(A, C, L) = 0$  in the remaining phases. Our calculations are consistent with this behavior but we found that the maximum in  $c(A, C, L)$  does not provide an accurate procedure to locate the critical couplings since it is rather flat within a wide range of couplings near  $u = 0$ . To obtain an estimate of the central charge  $c$  at criticality we first accurately locate the critical couplings using the non-linear fitting of Eq. (12) and extract a size-dependent  $c(L)$  from the singular part of the free energy in Eq. (15), which is subsequently extrapolated to  $L \rightarrow \infty$ .

## V. ESTIMATES OF CRITICAL POINTS, EXPONENTS AND CONFORMAL ANOMALIES

We computed eigenvalues of the transfer matrix for various points along the critical curve and used these to extract estimates for the central charge. In two cases we recomputed the critical points themselves from a scaling analysis of the interface free energy and helicity modulus. We start our discussion with the latter. Fig. 3 is a scaling plot of the Ising interface free energy as a function of  $A$  at fixed  $C = 0.2885$ . Fig. 4 is the same for  $XY$  interface, obtained by choosing boundary conditions that induce a twist of  $\pi$  in the  $XY$

variables. Figs. 5 and 6 are analogous plots for the case  $A = 2$  with varying  $C$ . The scaling plots for the systems with anti-periodic boundary conditions in the Ising variables do not display statistically significant deviations from the scaling hypothesis. However, this is not the case for the scaling plots for systems with a twist in the  $XY$  variables as shown most clearly by Fig. 4. In fact, significant changes are, e.g. in the critical amplitude, are observed in the “scaling plot” if smaller system sizes are omitted from the fit.

In all cases, there are strong corrections to scaling for small systems. This is demonstrated in Figs. 7 and 8, plots of the estimated effective critical couplings versus inverse system size. The effective coupling associated with size  $L$  was obtained by a least-squares fit to system sizes including sizes  $L$  and up.

By extrapolation assuming overly conservative  $1/L^2$  corrections, we obtain the following estimated critical points:  $A = 1.0014$  (Ising twist) and  $A = 1.0025$  ( $XY$  twist) at  $C = 0.2885$ , where the first of these two is presumably the more reliable one. Similarly, for  $A = 2$  the results are  $C = 1.318$  (Ising twist) and  $C = 1.316$  ( $XY$  twist). Our estimates for the critical exponents are summarized in Table I; the plots in Figs. 7 and 8 may serve to provide rough error bars.

Finally, we estimated the conformal anomaly  $c$  along the critical line using Eq. (15) and taking 2, 3 or 4 consecutive system sizes. This defines an effective  $c(L)$  at  $L^{-1} = (L_{\min}^{-1} + L_{\max}^{-1})/2$ , where  $L_{\min}$  and  $L_{\max}$  are the smallest and largest size used in the fit. Critical points not mentioned above, *viz.* ( $A = 3$ ,  $C = -2.3250$ ) and ( $A = 0.6$ ,  $C = 0.1520$ ), were taken from the estimates provided in Refs. 1 and 2. The results are summarized in Fig. 13.

## VI. DISCUSSION

The results obtained from the Ising interface free energy, summarized in Table I, seem sufficiently accurate to exclude pure Ising critical exponents ( $y_T = 1$  and  $y_I^{(d)} = 15/8$ ) for the point  $A \approx 1$ . Our numerical results agree with those for the 19-vertex model obtained by Knops *et al.*<sup>14</sup>, who find  $y_T = 1.23(3)$  and  $y_I^{(d)} = 1.80(1)$ . Within the sizable uncertainties

in the estimates of the same exponents for  $A = 2$ , we find no evidence for variation of these exponents along the critical line. The results obtained for the thermal exponent  $y_T$  are consistent with those from direct Monte Carlo simulations<sup>2</sup> of the  $XY$ -Ising model: 1.19(4) for  $A = 1$  and  $y_T = 1.18(4)$  for  $A = 2$ . We note, however, that the latter computations indicate variation along the critical line of the scaling exponent of the order parameter, an exponent which was not computed in the present transfer matrix Monte Carlo approach. Lee *et al.* found:  $y_I^{(o)} = 1.85(2)$  for  $A = 1$  and  $y_I^{(o)} = 1.80(2)$ .

There is a serious internal inconsistency in our estimates for  $y_T$  as obtained from the Ising interface and those obtained from the  $XY$  interface. Although Figs. 9 and 10 display strong corrections to scaling, there is no indication that the two ways of computing this thermal exponent will become consistent in the limit of large systems. This calls in question the validity of the basic assumption of scaling theory, *viz.*, that there is a single divergent length scale in this system as the critical point is approached along a temperature-like direction.

The results for the critical exponents  $y_T$  and  $y_I^{(d)}$  for the  $XY$ -Ising model are consistent with similar Monte Carlo transfer matrix calculations for the FFX $Y$  model on a square lattice<sup>13</sup> ( $y_T = 1.25(6)$ ,  $y_I^{(d)} = 1.81(2)$ ) and its one-dimensional quantum version<sup>16</sup> ( $y_T = 1.24(6)$ ,  $y_I^{(d)} = 1.77(2)$ ), although the strip widths are much larger here and the accuracy much better. Estimates of the critical exponent  $y_T$  for the FFX $Y$  model obtained from Monte Carlo simulations<sup>2</sup>, 1.21(3) (square lattice) and 1.18(3) (triangular lattice) are also in good agreement with the result for the  $XY$ -Ising model and seem to support an  $XY$ -Ising universality class for these systems.

The exponent  $y_I^{(o)} = 1.85$  for the  $XY$ -Ising model obtained from Monte Carlo simulations<sup>2</sup> is significantly larger than the result for  $y_I^{(d)}$  in Table I. This discrepancy is also observed in the results for the FFX $Y$  model<sup>13,14</sup> and can in part be attributed to corrections due to the effective free boundary conditions for the  $XY$  degrees of freedom at criticality. As argued in the context of the FFX $Y$  model<sup>14</sup>, since the  $XY$  degrees of freedom are uncoupled across an Ising domain wall, the  $XY$  variables should be regarded as

having free boundary conditions instead of periodic ones. This results in a correction to the estimate of  $x^{(d)} \rightarrow x^{(d)} - 1/16$  which seems to improve the agreement between  $y_I^{(o)}$  and  $y_I^{(d)}$  although, as mentioned in Sec. IV, the precise relation between these exponents is not known.

The results for the exponents in Table I and the scaling plots for  $\mathcal{A}(u)$  for the interface free energies are based on the naive assumption that the  $XY$  and Ising correlation lengths behave as  $\xi_\alpha \sim t^{-1/y_\alpha}$  with  $y_\alpha$  determined by independent best fits for the Ising and  $XY$  interfacial free energies. Such a procedure would certainly be incorrect if the  $XY$  and Ising variables were decoupled as then  $\log \xi_{XY} \sim t^{-1/2}$ . In the present case, these degrees are strongly coupled and the appropriate scaling form is not known and the  $XY$  degrees of freedom are probably subject to large slowly decaying corrections-to-scaling making the analysis of the data fraught with difficulty and uncertainty. A detailed analysis of the data for the  $XY$  twist free energy shows that the estimates of the finite-size scaling parameters  $a_i$  of Eq.(12) are not stable and depend on the number of data points included in the fit. For this reason, the scaling plots of  $\mathcal{A}(u)$  are somewhat misleading and a naive use of Eq.(13) to estimate  $x_{XY}^{(d)}$  yields the  $L = 4$  value for  $y^{(d)} = 2 - x^{(d)}$  of Figs.(11,12). The reason behind this is that the small  $L$  data has the lowest  $\chi^2$  and is most heavily weighted in the scaling plots of Figs. 4 and 6. It is amusing to note that the use of these estimates together with the with the relation, valid for a self dual Gaussian model<sup>14</sup>,  $x_{XY,1/2}^{(d)} x_{XY,1}^{(o)} = 1/16$ , gives results in agreement with those of Knops et al<sup>14</sup>. However, we consider this to be fortuitous and not to be taken seriously. Another difficulty with analyzing numerical data for the  $XY$  twist free energy is that there must be a crossover to a low temperature Gaussian fixed line when  $u \gg 0$  as the low temperature phase must be just a  $XY$  model when there is long-range Ising order.

The well-known difficulties of analyzing numerical data for the helicity modulus in this system are compounded by this cross-over so it is not surprising that we are unable to make definitive statements about the critical exponents for the  $XY$  variables. One might try using a dual roughening representation, but there are negative Boltzmann weights at the critical



point in the dual representation which will lead to some difficulties. Despite being able to go to relatively large strip widths of  $L = 30$  we are unable to reach definite conclusions about the critical behavior of the  $XY$  degrees of freedom except to say that our simple ansatz for the scaling of the  $XY$  twist is inadequate and corrections to scaling should be included in the analysis, but we do not know the form these should take. Also, we are unable to estimate the discontinuity  $\pi\Delta\gamma$  in the helicity modulus except to say that, at the critical point  $\pi\gamma \approx 1.1$  and, at  $T_c^-$ ,  $\pi\Delta\gamma \approx 4$  which we believe to be a fairly realistic estimate.

We now consider the results for the central charge in Fig. 13. The results for  $A = 0.6$  correspond to the branch point in Fig. 1 as estimated from Monte Carlo simulations<sup>2</sup>. Convergence is very poor in this case. The effective  $c$  starts at  $c = 1.5$  for small systems, decreases very slowly for intermediate systems and then decreases rapidly for the largest system sizes. It is not possible to estimate the asymptotic value for this case. In fact, this behavior suggests inaccuracy in the estimate of the critical point. The other curves in Fig. 1 correspond to different points along the line of single transitions. Again, corrections to scaling are decaying too slowly as a function of system size to allow an accurate estimate of  $c$  in the large  $L$  limit. However,  $c = 3/2$  along the line is not inconsistent with the data. This is shown in Table II where the central charge is estimated assuming power-law corrections of the form  $\alpha/L^{3-s} + \beta/L^{4-s}$  the leading correction to the free energy,  $\pi c/6L^2$ , in Eq. 15. We chose  $s = 0.2$  so that we could simultaneously fit the results for  $A \approx 1$  and  $A = 2$ . This value,  $c = 3/2$ , would be the expected one if the critical behavior along the single line could be described as a superposition of critical Ising and  $XY$  models<sup>20</sup>. Our results for the critical exponents  $y_t$  and  $y_h$  however are not consistent with this hypothesis and suggest that the coupling between the Ising and  $XY$  degrees of freedom is vital. The results of the extrapolations should also be viewed with caution since they are not completely justified. There could be other corrections as  $\exp(-aL)$  or  $\ln L/L$  but due to the noise in the data any attempt to include such terms in the extrapolation is pointless.

## VII. CONCLUSIONS

We have obtained critical exponents and the central charge for the  $XY$ -Ising model using Monte Carlo transfer matrix calculations on infinite strips of widths  $L$  as large as 30 lattice spacings. The results for  $c$  show a significant decrease with increasing  $L$  but converge very slowly to an asymptotic value. An extrapolation procedure indicates that these values are not inconsistent with  $c = 3/2$ . However, on purely numerical grounds, we can not rule out the possibility of a larger value or even  $c$  varying along the line of single transitions. Our results for the central charge suggest that the recent estimates of this quantity for the related FFX $Y$  models are likely to be subject to similar systematic errors due to slowly decaying corrections-to-scaling and the asymptotic value is consistent with  $c = 3/2$ . The critical exponents associated with Ising-like order parameter are obtained more accurately and are found to be significantly different from the pure Ising values but are consistent with previous Monte Carlo simulations which suggested new critical behavior and also with recent estimates for the FFX $Y$  model using Monte Carlo and exact transfer matrix calculations.

## ACKNOWLEDGMENTS

We thank H.W.J. Blöte and J. Lee for many helpful discussions. E.G. was supported by Fundação de Amparo à Pesquisa do Estado de São Paulo (FAPESP, Proc. No. 92/0963-5) and Conselho Nacional de Desenvolvimento Científico e Tecnológico (CNPq). J.M.K. was supported by the NSF under Grants DMR-9222812 and NSF-INT-9016257 and M.P.N. by DMR-9214669 and CHE-9203498. This research was conducted in part using the resources of the Cornell Theory Center, which receives major funding from the National Science Foundation (NSF) and New York State, with additional support from the Advanced Research Projects Agency (ARPA), the National Center for Research Resources at the National Institutes of Health (NIH), IBM Corporation, and other members of the center's Corporate Research Institute.

## REFERENCES

- <sup>1</sup> E. Granato, J.M. Kosterlitz, J. Lee and M.P. Nightingale, Phys. Rev. Lett. **66**, 1090 (1991).
- <sup>2</sup> J. Lee, E. Granato and J.M. Kosterlitz, Phys. Rev. B **44**, 4819 (1991).
- <sup>3</sup> J. Villain, J. Phys. C **10**, 4793 (1977).
- <sup>4</sup> S. Teitel and C. Jayaprakash, Phys. Rev. B **27**, 598 (1983).
- <sup>5</sup> S. Miyashita and H. Shiba, J. Phys. Soc. Jpn. **53**, 1145 (1984).
- <sup>6</sup> M.Y. Choi and S. Doniach, Phys. Rev. B **31**, 4516 (1985).
- <sup>7</sup> M. Yosefin and E. Domany, Phys. Rev. B **32**, 1778 (1985).
- <sup>8</sup> E. Granato, J.M. Kosterlitz, J. Phys. C **19**, L59 (1986); J. Appl. Phys. **64**, 5636 (1988).
- <sup>9</sup> E. Granato, J. Phys. C **20**, L215 (1987).
- <sup>10</sup> J.M. Thijssen and H.J.F. Knops, Phys. Rev. B **37**, 7738 (1988).
- <sup>11</sup> J.M. Thijssen and H.J.F. Knops, Phys. Rev. B **42**, 2438 (1990).
- <sup>12</sup> G. Ramirez-Santiago and J.V. José, Phys. Rev. Lett. **68**, 1224 (1992).
- <sup>13</sup> E. Granato and M.P. Nightingale, Phys. Rev. B **48**, 7438 (1993).
- <sup>14</sup> Y.M.M. Knops, B. Nienhuis, H.J.F. Knops and H.W.J. Blöte, Phys. Rev. B **50**, 1061, (1994).
- <sup>15</sup> S. Teitel and C. Jayaprakash, Phys. Rev. Lett. **51**, 199 (1983).
- <sup>16</sup> E. Granato, Phys. Rev. B **45**, 2557 (1992); *ibid.* **48**, 7727 (1993).
- <sup>17</sup> M. den Nijs, Phys. Rev. B **32**, 4785 (1985).
- <sup>18</sup> M. den Nijs, Phys. Rev. B **46**, 10386 (1992).

- <sup>19</sup> J. Lee, J.M. Kosterlitz and E. Granato, Phys. Rev. B **43**, 11531 (1991).
- <sup>20</sup> O. Foda, Nucl. Phys. **B300**, 611 (1988).
- <sup>21</sup> M.P. Nightingale, in *Finite-Size Scaling and Numerical Simulation of Statistical Systems*, edited by V. Privman (World Scientific, Singapore, 1990).
- <sup>22</sup> M.P. Nightingale and H. W. J Blöte, unpublished.
- <sup>23</sup> J.L. Cardy, J. Phys. A. **17**, L961 (1984).
- <sup>24</sup> H.W. Blöte, J.L. Cardy and M.P. Nightingale, Phys. Rev. Lett. **56**, 742 (1986).
- <sup>25</sup> A.B. Zamolodchikov, Pis'ma Zh. Eksp. Teor. Fiz. **43**, 567 (1986) [JETP Lett. **43**, 733 (1986)].

## Table Captions

1. Critical exponents associated with the variables for which the boundary conditions were twisted.
2. Estimates of the central charge  $c$  assuming the free energy per site to be of the form  $f_\infty + \frac{\pi c}{6L^2} + \frac{\alpha}{L^{2.8}} + \frac{\beta}{L^{3.8}}$ . Fits were made using data for  $L, L+2, \dots, 30$ . For  $L \geq 10$ ,  $\beta$  was fixed at the value obtained from the  $L=4$  fit. In all cases the normalized  $\chi^2$  was of order unity.

## Figure Captions

1. Phase diagram of the  $XY$ -Ising model<sup>1,2</sup>. Solid and dotted lines indicate continuous and first-order transitions, respectively. Filled circles indicate the locations where the present calculations were performed.
2. Left: graphical representation of the conditional partition function of a semi-infinite strip with helical boundary conditions, i.e., the left eigenvector of the transfer matrix, which is shown on the right. In the lattice on the left, open circles represent sites with variables  $t_i$  and  $n_i$  ( $i = 1, \dots, L$ ) that specify the surface configuration upon which the conditional partition function depends. The full circles represent sites with variables that have been summed over. Right: graphical representation of the transfer matrix. The variables associated with the circles make up the left index of the matrix; the dots go with the right index. Coincidence of a circle and a dot produces a product of two  $\delta$ -functions.
3. Scaling plot of the interfacial free energy with Ising-twisted boundary conditions;  $A \approx 1$  is varied at constant  $C = 0.2885$ .
4. Scaling plot of the interfacial free energy with  $XY$ -twisted boundary conditions;  $A \approx 1$  is varied at constant  $C = 0.2885$ .

5. Scaling plot of the interfacial free energy with Ising-twisted boundary conditions;  $C \approx 1.32$  is varied at constant  $A = 2$ .
6. Scaling plot of the interfacial free energy with  $XY$ -twisted boundary conditions;  $C \approx 1.32$  is varied at constant  $A = 2$ .
7. Effective critical couplings  $A_c$  vs.  $1/L$  and the results of extrapolation to  $L = \infty$  at  $C = 0.2885$  for both boundary conditions.
8. Effective critical coupling  $C_c$  vs.  $1/L$  and the results of extrapolation to  $L = \infty$  at  $A = 2$  for both boundary conditions.
9. Effective  $y_T$  vs.  $1/L$  for critical point at  $A \approx 1$ .
10. Effective  $y_T$  vs.  $1/L$  for critical point at  $A = 2$ .
11. Effective  $y^{(d)}$  vs.  $1/L$  for critical point at  $A \approx 1$ .
12. Effective  $y^{(d)}$  vs.  $1/L$  for critical point at  $A = 2$ .
13. Effective conformal anomaly vs inverse system size  $1/L$  for various values of  $A$ .

TABLES

TABLE I. Critical exponents associated with the variables for which the boundary conditions were twisted.

	Ising	$XY$
$A \approx 1$	$y_T = 1.27$ $y_1^{(d)} = 1.798$	$y_T = 0.97$ $y_{XY, \frac{1}{2}}^{(d)} = 1.715$
$A = 2$	$y_T = 1.45$ $y_1^{(d)} = 1.801$	$y_T = 1.12$ $y_{XY, \frac{1}{2}}^{(d)} = 1.616$

TABLE II. Estimates of the central charge  $c$  assuming the free energy per site to be of the form  $f_\infty + \frac{\pi c}{6L^2} + \frac{\alpha}{L^{2.8}} + \frac{\beta}{L^{3.8}}$ . Fits were made using data for  $L, L + 2, \dots, 30$ . For  $L \geq 10$ ,  $\beta$  was fixed at the value obtained from the  $L = 4$  fit. In all cases the normalized  $\chi^2$  was of order unity.

	$L$	$c$
$A \approx 1$	4	1.466(6)
	6	1.47(1)
	8	1.44(4)
	10	1.46(1)
	12	1.46(2)
$A = 2$	4	1.62(2)
	6	1.57(4)
	8	1.48(9)
	10	1.57(3)
	12	1.56(6)

FIGURES

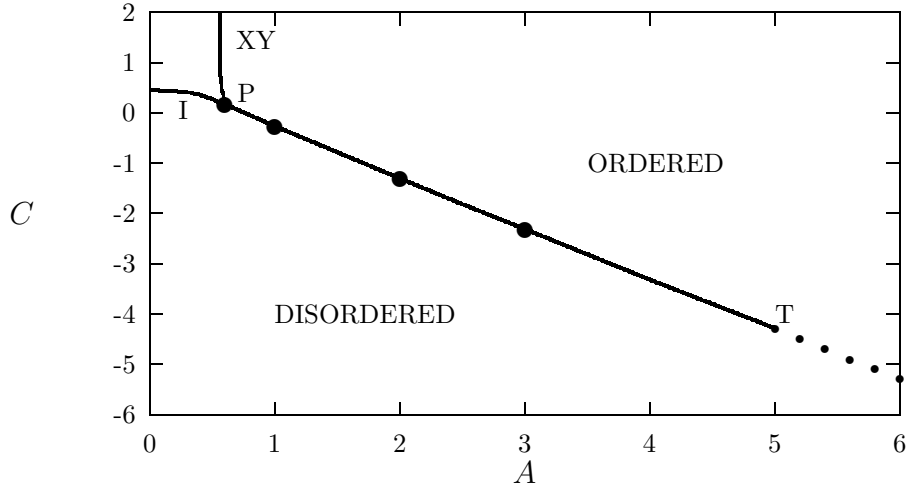


FIG. 1. Phase diagram of the XY-Ising model<sup>1,2</sup>. Solid and dotted lines indicate continuous and first-order transitions, respectively. Filled circles indicate the locations where the present calculations were performed.

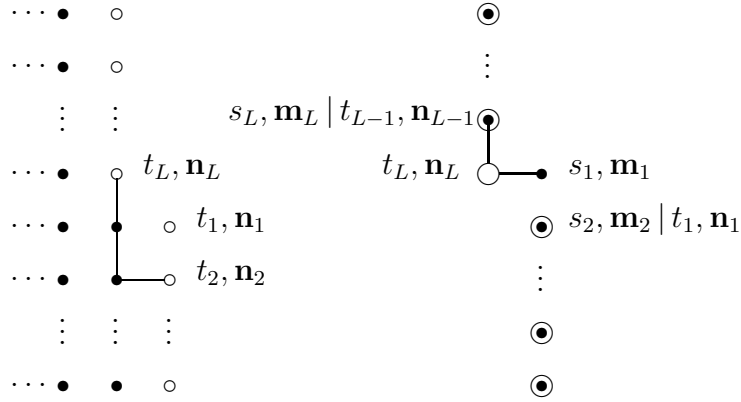




FIG. 2. Left: graphical representation of the conditional partition function of a semi-infinite strip with helical boundary conditions, i.e., the left eigenvector of the transfer matrix, which is shown on the right. In the lattice on the left, open circles represent sites with variables  $t_i$  and  $n_i$  ( $i = 1, \dots, L$ ) that specify the surface configuration upon which the conditional partition function depends. The full circles represent sites with variables that have been summed over. Right: graphical representation of the transfer matrix. The variables associated with the circles make up the left index of the matrix; the dots go with the right index. Coincidence of a circle and a dot produces a product of two  $\delta$ -functions.

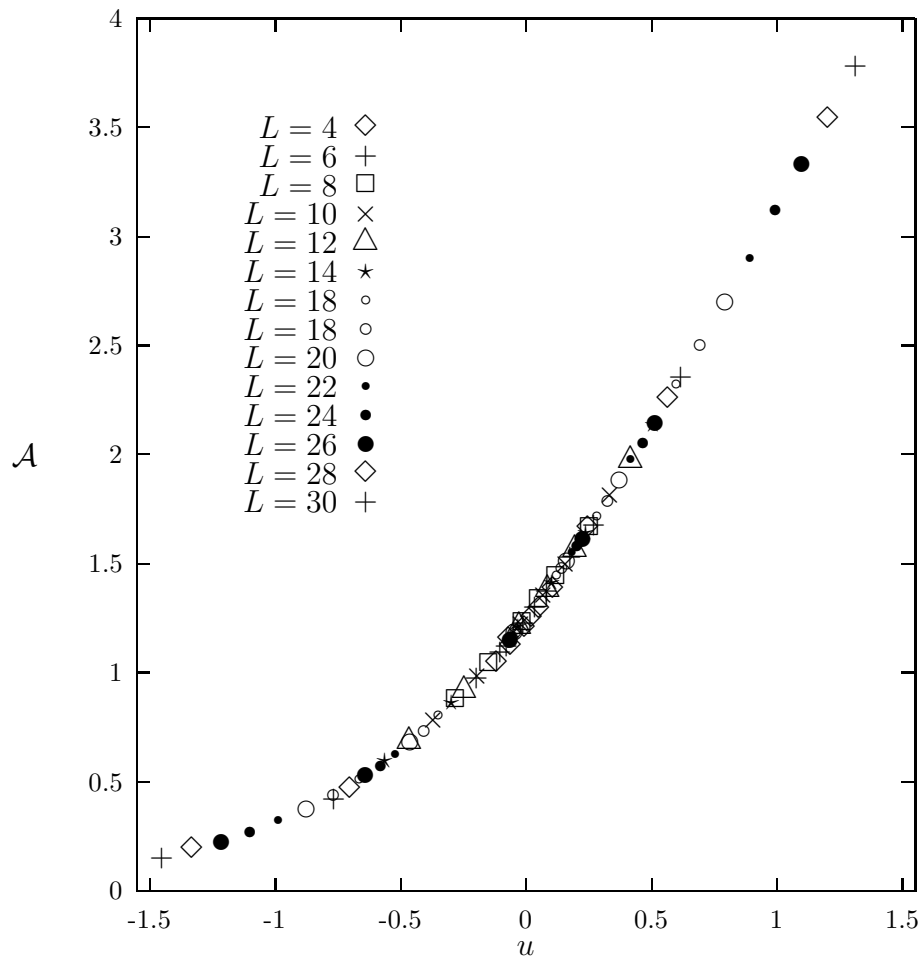


FIG. 3. Scaling plot of the interfacial free energy with Ising-twisted boundary conditions;  $A \approx 1$  is varied at constant  $C = 0.2885$ .

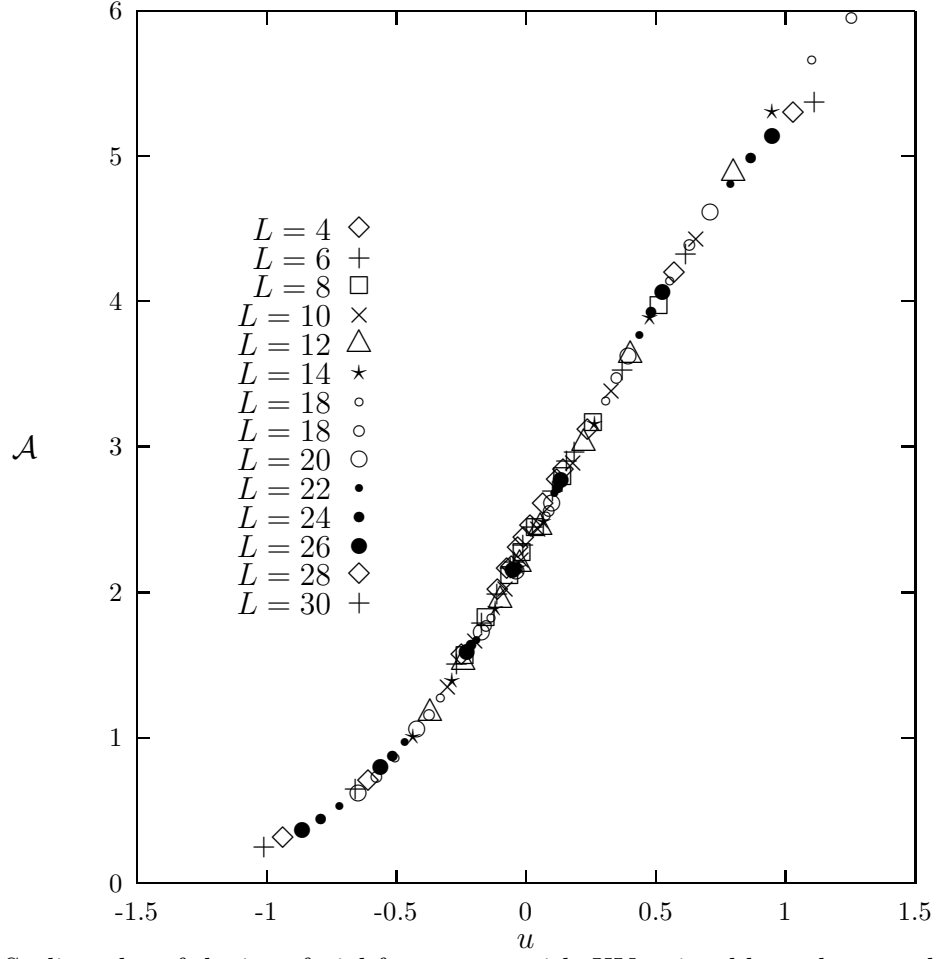


FIG. 4. Scaling plot of the interfacial free energy with  $XY$ -twisted boundary conditions;  $A \approx 1$  is varied at constant  $C = 0.2885$ .

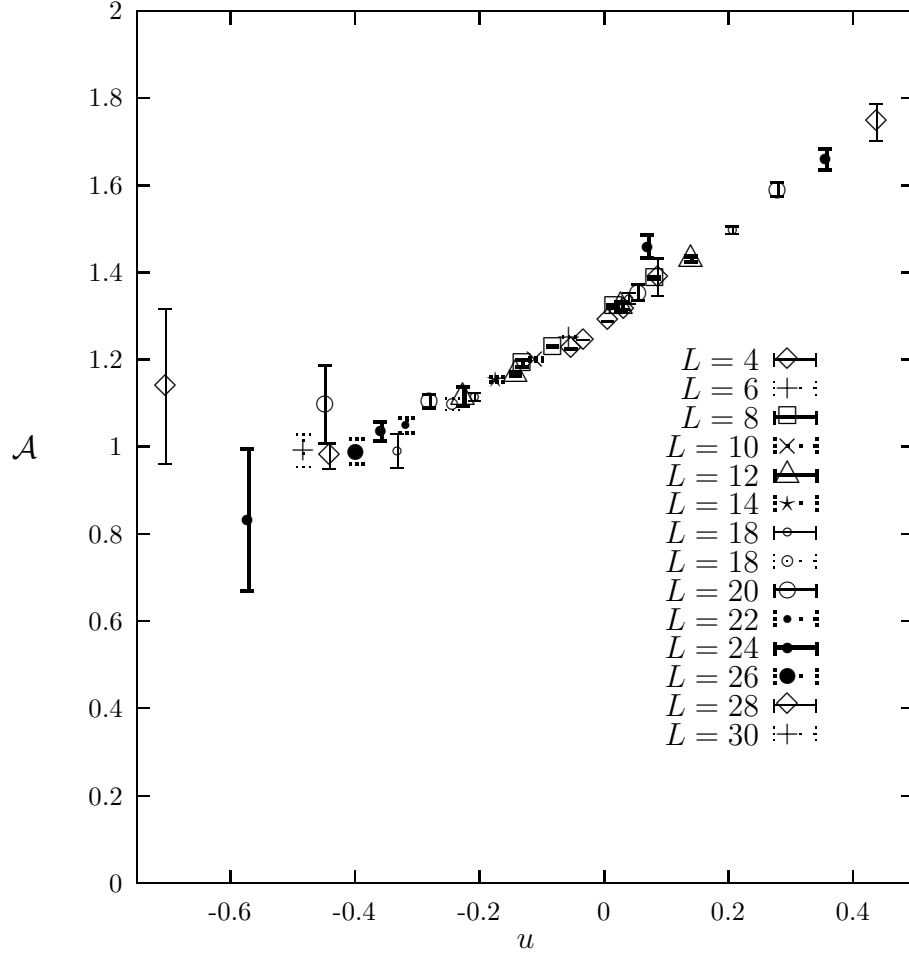


FIG. 5. Scaling plot of the interfacial free energy with Ising-twisted boundary conditions;  $C \approx 1.32$  is varied at constant  $A = 2$ .

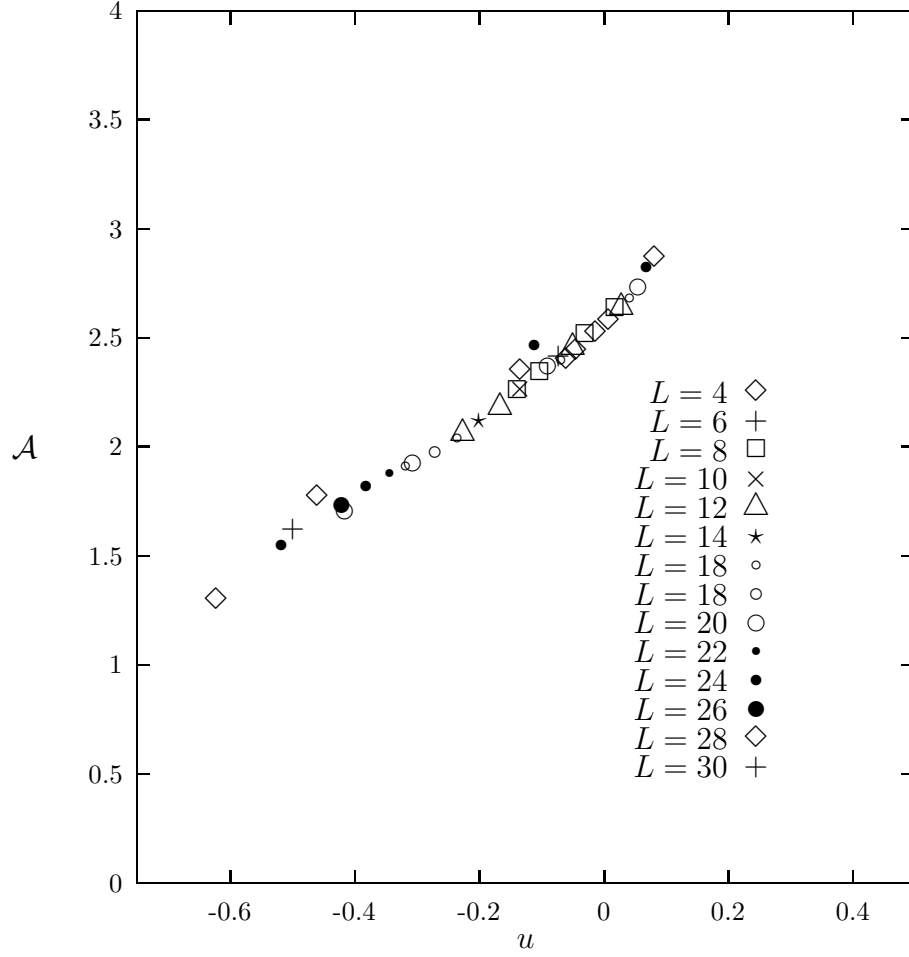


FIG. 6. Scaling plot of the interfacial free energy with  $XY$ -twisted boundary conditions;  $C \approx 1.32$  is varied at constant  $A = 2$ .

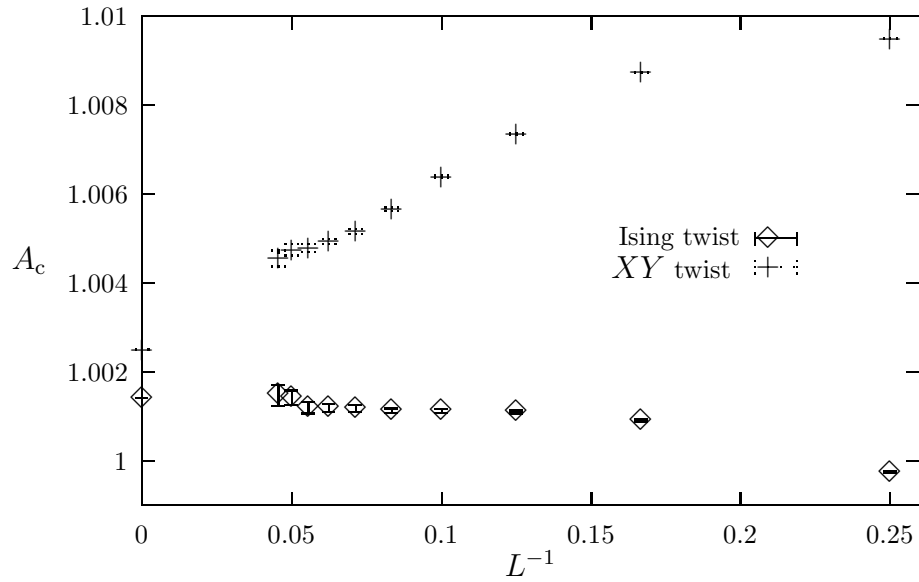


FIG. 7. Effective critical couplings  $A_c$  vs.  $1/L$  and the results of extrapolation to  $L = \infty$  at  $C = 0.2885$  for both boundary conditions.

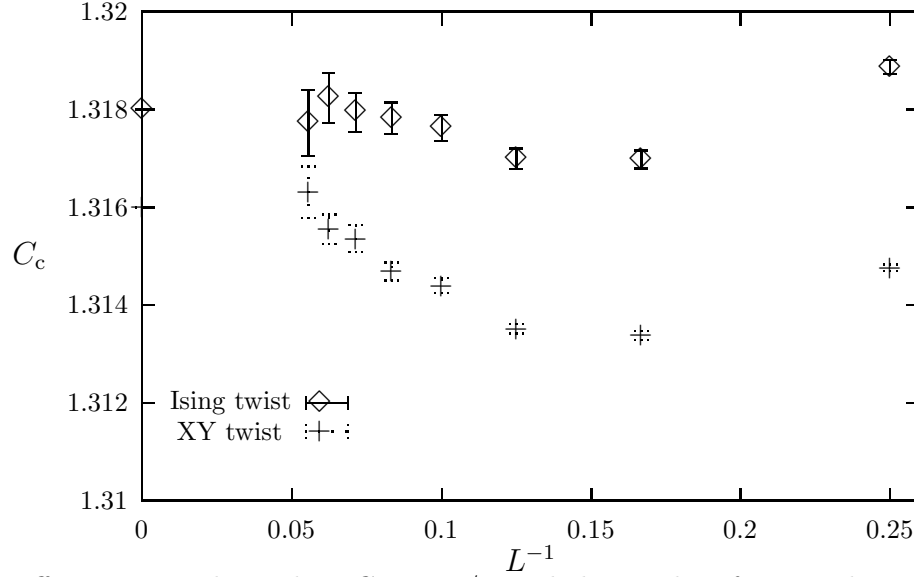


FIG. 8. Effective critical coupling  $C_c$  vs.  $1/L$  and the results of extrapolation to  $L = \infty$  at  $A = 2$  for both boundary conditions.

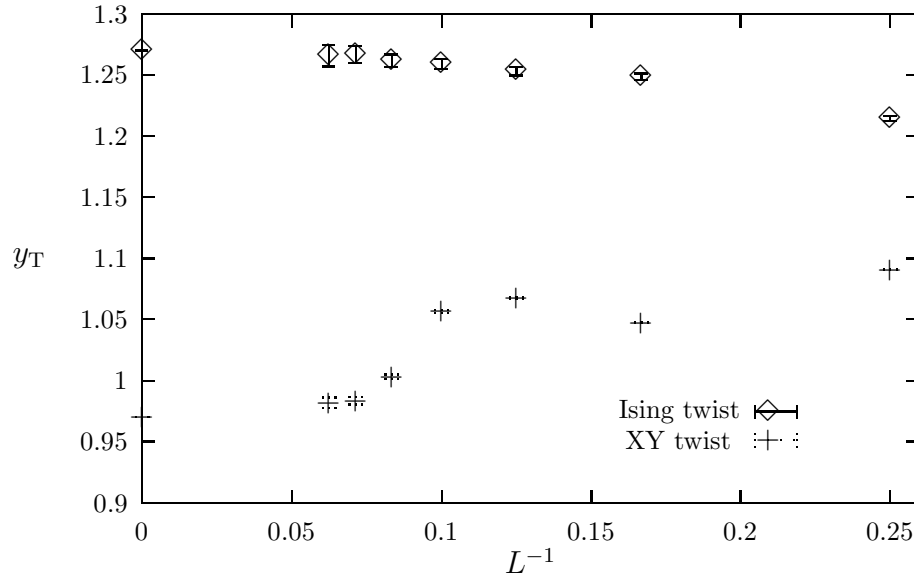


FIG. 9. Effective  $y_T$  vs.  $1/L$  for critical point at  $A \approx 1$ .

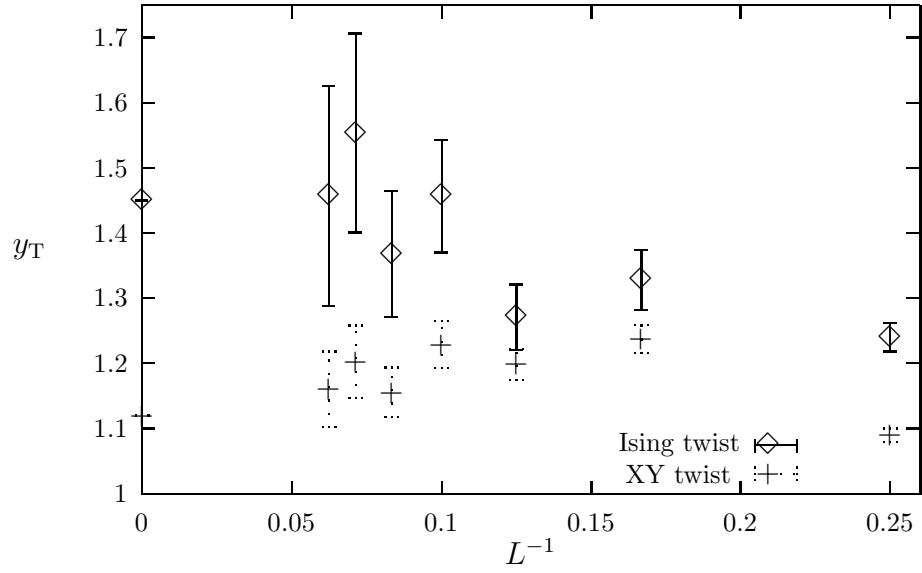


FIG. 10. Effective  $y_T$  vs.  $1/L$  for critical point at  $A = 2$ .

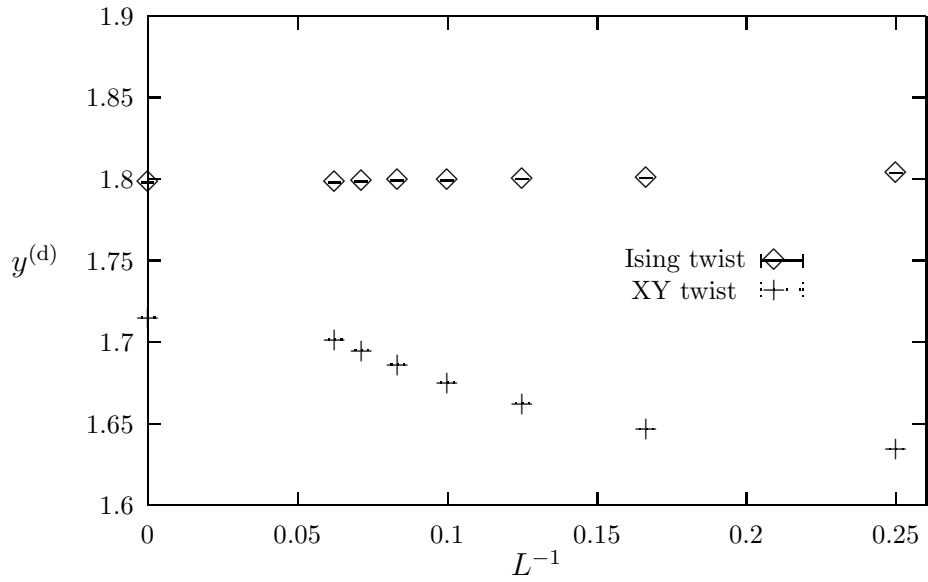


FIG. 11. Effective  $y^{(d)}$  vs.  $1/L$  for critical point at  $A \approx 1$ .

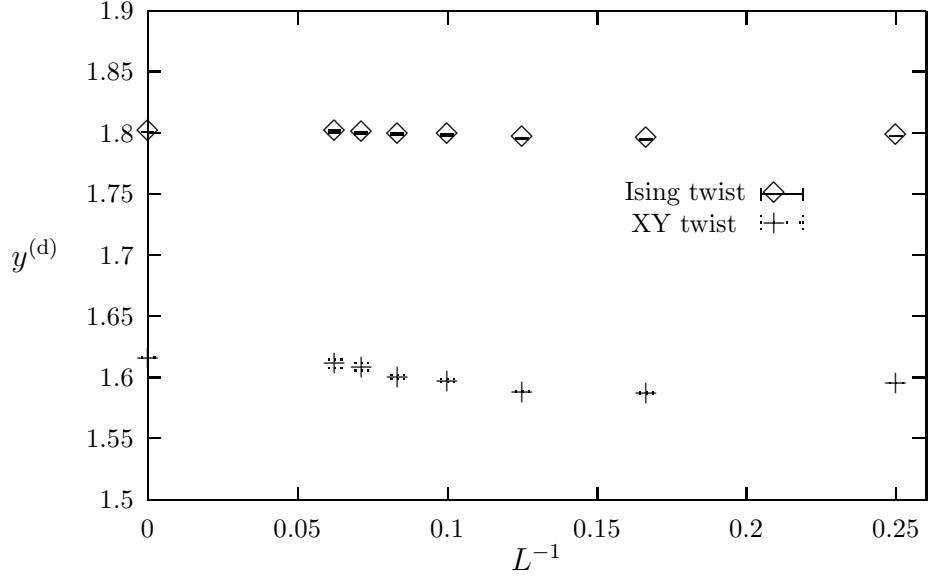


FIG. 12. Effective  $y^{(d)}$  vs.  $1/L$  for critical point at  $A = 2$ .

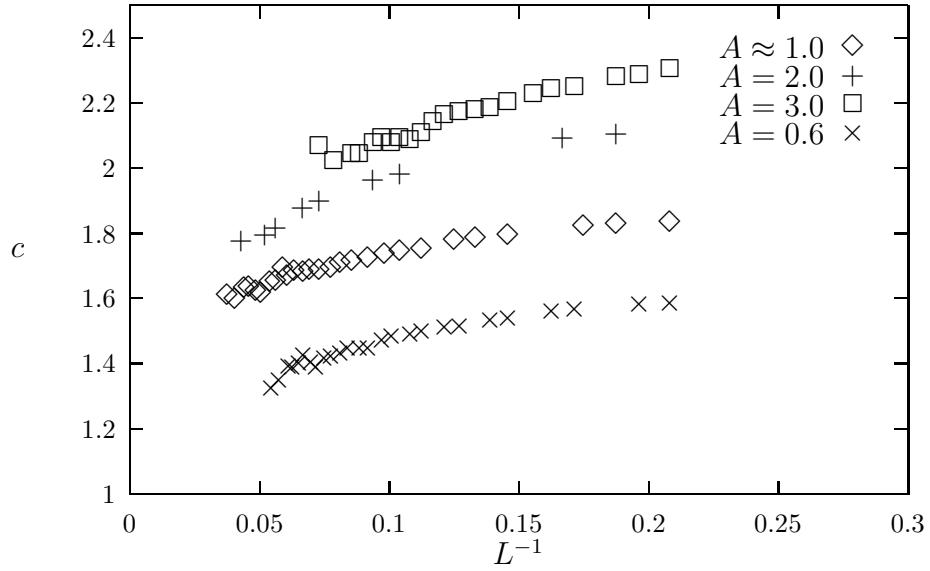


FIG. 13. Effective conformal anomaly vs inverse system size  $1/L$  for various values of  $A$